Characterization of the Surface Integrity induced by Hard Turning of Bainitic and Martensitic AISI 52100 Steel

Available online at www.sciencedirect.com

SciVerse ScienceDirect

Procedia CIRP 1 (2012) 494 – 499

www.elsevier.com/locate/procedia

5th CIRP Conference on High Performance Cutting 2012

Characterization of the Surface Integrity induced by Hard Turning of Bainitic and Martensitic AISI 52100 Steel

S. B. Hosseini[a*], K. Ryttberg[b], J. Kaminski[a], U. Klement[a]

[a]*Department of Materials and Manufacturing Technology, Chalmers University of Technology, SE-412 96 Gothenburg, Sweden*

[b]*SKF Sweden AB, SE-415 50 Gothenburg, Sweden*

* Corresponding author. Tel.: +46-31-337-2854.E-mail address: seyed.hosseini@chalmers.se

Abstract

Depending on the process parameters and the tool condition, hard turned surfaces can consist of a "white" and a "dark" etching layer having other mechanical properties compared to the bulk material. X-ray diffraction measurements revealed that tensile residual stresses accompanied with higher volume fraction of retained austenite are present in the thermally induced white layer. While compressive residual stresses and decreased retained austenite content was found in the plastically created white layer. The surface temperature was estimated to be ~1200˚C during white layer formation by hard turning.

Keywords: Surface integrity; White layer; Hard machining; X-ray diffraction; Scanning electron microscopy

1. Introduction

Hard turning (> 45 HRC) has over the last decades become both a complementing and a replacing process to grinding. Some of the advantages with hard turning are surface integrity similar to grinding, dry cutting possibilities and greater flexibility for complex geometries [1]. Moreover, the process is also considered to be more sustainable due to lower energy consumption [1]. Surface roughness values down to Ra = 0.14 µm after conducting hard turning as a surface finishing operation has been obtained [2].

By controlling the cutting parameters and with proper selection of the cutting inserts, it is possible to tailor the surface integrity of the component in order to achieve beneficial stress profiles and acceptable topographical and metallurgical surface properties [3]. Like many other cutting processes, the tool wear (flank and crater wear) in hard turning has a significant influence on the final surface integrity. Both the physical properties and the functional behaviour of the surface are significantly altered with the progress of tool wear.

Tonshoff et al. [4] showed that an increase in the flank wear will alter the residual stress profile from beneficial to detrimental state and lead to the formation of both a "white" and a "dark" etching layer with inferior topographical properties. The phenomenon of white layer formation was observed for the first time by Stead [5] who observed it on steel wire ropes. Later, Griffiths [6] suggested three different mechanisms for the formation of the white layers: i) plastic deformation producing a homogenous structure or a layer with very fine grain size, ii) rapid heating followed by rapid cooling resulting in a phase transformation and iii) surface reaction with the environment. The "dark" etching layer is often called the over-tempered layer and possesses a somewhat lower hardness than the bulk material. Thiele et al. [7] studied the effect of cutting edge geometry and work material hardness upon the surface integrity of AISI 52100. They showed that large edge honed tools produce more compressive residual stresses and continuous white layers as compared to small edge honed tools. The heating of the surface above the α-γ transformation temperature and subsequent rapid cooling was described as the main mechanism for the

 http://dx.doi.org/10.1016/j.procir.2012.04.088

white layer formation accompanied with compressive residual stresses. The retained austenite content in the white layer was reported by Ramesh et al. [8] to vary with the cutting speed. The lowest retained austenite content was obtained for the sample cut with lowest cutting speed (91.4 m/min) where severe plastic deformation was held as responsible for the white layer formation. Ackan et al. [9] reported that the retained austenite content in the white layer was less than 10 vol.%. However, no information of the retained austenite content prior to machining was given. High degree of plastic deformation accompanied by dynamic recrystallization and cementite dissolution was suggested as the main mechanisms for formation of white layer [9]. Tönshoff et al. [4], who studied the formation of white layer in case hardened steel (DIN 16MnCr5), reported high surface tensile stresses down to a depth of 20 µm (V_B = 0,2 mm). The white layer was reported to mainly consist of retained austenite, which they based upon the intensity differences in the austenitic/ferritic peaks obtained by X-ray diffraction before and after machining. In the present investigation, the effect of flank wear and cutting speed on the white and dark layer formation was systematically studied. The microstructure of white and dark layer has been characterized by means of scanning electron microscopy. The residual stress patterns as well as the retained austenite content in the white layers were studied using X-ray diffraction. Based on the white layer constituents the surface temperature which must be reached during white layer formation was estimated.

2. Materials and Methods

The chemical composition of the cylindrical steel bars is given in Table 1. Two different heat treatments were carried out in order to obtain test materials containing either a martensitic (M1-M6) or a bainitic (B1-B6) microstructure. Prior to final hardening treatment, the microstructure of the steel consisted of evenly distributed spheroidized $(Fe,Cr)_3C$ carbides in a ferritic matrix with a hardness of ~200 HV30. The hardness of the martensitic and the bainitic microstructures were 747±10 and 715±12 HV30. The surface and subsurface residual stresses were determined by means of X-ray diffraction with a XSTRESS 3000 G2R diffractometer equipped with a Cr-Kα source. For the residual stress measurements, standard Psi (ψ) method was used with four equi-$\sin^2\psi$ tilts from -45˚/+45˚. The layer removal method was used to measure subsurface residual stresses. The retained austenite content was determined using a Bruker D8 Advance diffractometer, equipped with Cr-Kα source and an incident parabolic mirror. Stepwise increase in the grazing incidence angle reveal the existing gradient of the retained austenite content as well as structural changes. The hkl-planes $\{200\}_\gamma$, $\{220\}_\gamma$, $\{110\}_\alpha$, $\{200\}_\alpha$ were used for the retained austenite measurements. Split-PseudoVoigt was used in the software Topas V.4.2 to perform the curve fitting, where the maximum intensities from each peak were addressed for determination of the retained austenite content. Incident angles of 1˚, 2˚, 3˚ and 5˚ resulted in the penetration depths, 0.46, 0.91, 1.35 and 2.15 µm calculated with the software AborbDX V.1.1.4. The 2θ scan ranged between 64˚ to 160˚ with 0.02˚ in 2θ/step.

Table 1: Chemical composition of AISI 52100 steel.

Material	C	Mn	Si	Cr	S	P
AISI 52100	0.95	0.32	0.26	1.42	0.001	0.009

3. Experimental

During machining, the flank wear and the cutting speed were varied in a systematic way in order to obtain either predominantly mechanically or thermally induced white layers. Even though the created white layers will always be due to a combined effect of both mechanical work and thermal energy input, the process parameters may be chosen to favour one of the mechanisms. For example, with low cutting speed and high flank wear the thermal energy input will be suppressed while the mechanical work will be promoted. Figure 2a provides a graph of the cutting parameters used during the hard turning. Rhombic shaped CBN inserts of grade BNX10 (DCGW11T308) were utilized with a 0.12/-25˚ chamfer, 7˚ clearance angle and with a 0.8 mm nose radius. The flank wear on the inserts were induced by using the inserts on dummy specimens with comparable diameter and properties prior to the final cut. Cutting forces were measured with a piezoelectric force dynamometer. A water based cutting fluid containing 5% emulsion was applied on the rake side with a pressure of 5 bars. The depth of cut was set to 0.08 mm (DoC) and the feed rate (f) was chosen to be 0.08 mm/rev during the tests.

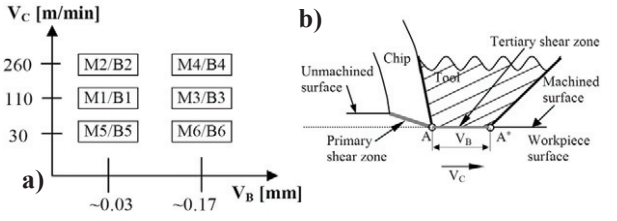

Fig. 2. a) Cutting speeds and flank wear used during hard turning tests. b) Schematic illustration of the interaction length A-A* between the workpiece surface and the tool flank wear.

4. Results

4.1. White layer and Dark Layer Thicknesses

The hard turning tests conducted for both materials revealed that the thickest white layer was obtained with the highest cutting speed combined with the highest flank wear. The white layer was followed subsequently by a dark layer as shown in Fig. 3a. The medium cutting speed resulted in a thinner white layer and a thicker dark layer. In the cutting zone on the tool flank side, the distance A-A* in Fig. 2b slides against the surface workpiece under high pressure and temperature. Having the value of the tool flank wear, V_B, and the cutting speed, V_C, it is possible to calculate the time when a certain point on the workpiece passes along the tool flank. For example, the highest cutting speed in combination with the highest flank wear gives a contact time of $t \approx 40$ µs while the medium cutting speed provides a contact time of $t \approx 95$ µs. Even when the flank wear was low (new insert), formation of white layer was observed on the surfaces machined with the highest cutting speed. The white layer created with these cutting conditions was discontinuous with a thickness up to 0.5 µm. Discontinuous white layer was also created with the lowest cutting speed and highest flank wear having a thickness of up to ~1 µm. Despite that the white layer was observed on the surfaces machined with the lowest cutting speed, no dark layer was detected. The white and dark layer thicknesses and the contact times between the tool flank side and the workpiece are given in Table 2. Examples of the fine microstructure of the white layer are given in the SEM figures in Fig. 3b-d.
Table 2: White and dark layer thicknesses and contact times (A-A*).

Table 2: White and dark layer thicknesses and contact times (A-A*).

Parameter	**M1**	**M2**	**M3**	**M4**	**M5**	**M6**
White layer [µm]	-	≤ 0.5	1.5±0.5	3±1.0	-	1±0.5
Dark layer [µm]	2±0.5	2±0.5	10±2.0	5±1.0	-	-
Contact time [µs]	16	7	95	40	60	350
	B1	**B2**	**B3**	**B4**	**B5**	**B6**
White layer [µm]	-	≤ 0.5	1.5±0.5	3±1.0	-	1±0.5
Dark layer [µm]	2±0.5	2±0.5	10±2.0	6±2.0	-	-
Contact time [µs]	16	7	95	40	60	350

4.2. Retained Austenite

Figure 4 shows the retained austenite contents after machining. Samples M5, M6 and B5, B6 are excluded from Fig. 4 since no austenite was detected. The variation of the retained austenite content from the surface down to a depth of ~2 µm is shown. In order to estimate the gradient of the retained austenite content, the measured volume fraction of the austenite phase from the previous layer was subtracted from the results in the subsequent layer. For example in sample M3, the retained austenite content measured with 1˚ incidence angle was estimated to be ~13 vol.% while it was ~10 vol.% at 2˚ incidence. When subtracting the information in layer 1 from layer 2, the revised retained austenite content for layer 2 became ~8 vol.%. Generally, the white layer created with originally martensitic microstructure contained higher amount of retained austenite than the white layer created with originally bainitic microstructure. It should be noted that the hard turned surfaces with lowest cutting speed did not show any austenite peaks in the X-ray diffraction pattern.

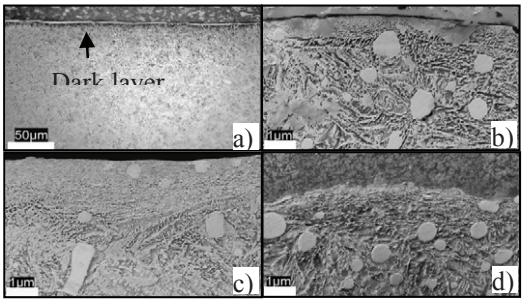

Fig. 3. a) Light optical microscopy image of white and dark layers. Scanning electron microscopy images of the white layer and the undissolved $(Fe,Cr)_3C$ in samples b) M3, c) M4 and d) M6.

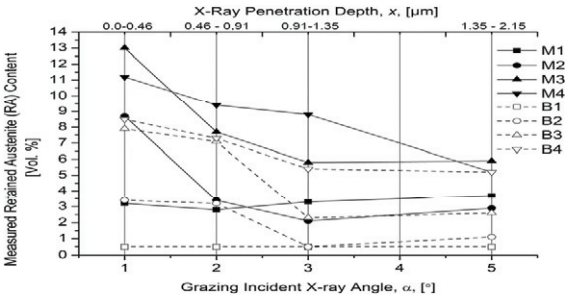

Fig. 4. Measured and corrected retained austenite content in white layer. The retained austenite content in sample B1 was less than 1% and therefore the expected values after heat treatment are included in the diagram.

4.3. Residual Stresses

As seen in Fig. 5a, the surfaces machined with new inserts and with medium or high cutting speeds were characterized by surface compressive residual stresses with their maximum compressive stresses at a depth of ~5 µm. The main changes observed in the residual stress profiles using worn inserts (Fig. 5b) at medium or high cutting speeds were 1) high surface tensile residual stresses and 2) the maximum compressive subsurface residual stresses were shifted towards larger depths,

~15-20 µm. The surfaces machined with lowest cutting speed had its maximum compressive residual stresses at the surface, while using a worn insert the maximum compressive stresses were shifted to larger depths, ~20-50µm. In axial direction the surface stresses were characterized by high compressive residual stresses, while in tangential direction the surface stresses were tensile. Generally, increased cutting speeds result in higher temperatures both in primary and tertiary zone even though the majority of the heat dissipates into the chips. As shown in this investigation, higher temperature influences both the surface and the subsurface residual stresses. However, the changes in the residual stress profiles were more pronounced when using a worn tool due to the increased thermo-mechanical effect (longer interaction distance). Where the subsurface maximum compressive residual stresses were shifted to greater depths, higher surface residual stresses were measured.

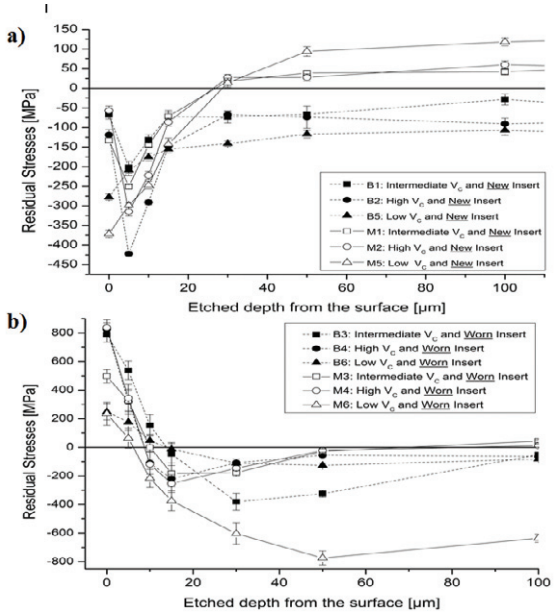

Fig.5. Measured residual stresses in the a) axial and b) tangential directions new and worn inserts for both materials.

5. Discussion

White layer formation requires a certain thermo-mechanical condition whether it is predominantly thermally or mechanically created. For example, this condition was not fulfilled for the surfaces machined with medium cutting speed and new inserts. Even though no white layer was detected, a dark etching layer (over tempered layer) was observed at the machined surfaces indicating that the temperature had been high enough to affect the surfaces. Increasing the cutting speed, the thermo-mechanical condition was promoted, resulting in a discontinuous and thin (0.5µm) white layer. Adding the additional effect from the flank wear, a thicker and continuous white layer (1.5 to 3 µm) was created. As shown in the Fig. 5, the increased tool flank wear shifted the position of the maximum compressive residual stresses to larger depths due to increased subsurface mechanical work. Similar behavior has been observed after studying the effect of tool edge geometry on the residual stresses where Thiele et al. [10] concluded that the presence of significant subsurface flow resulted in more compressive residual stresses. Since the white layer created at medium and high cutting speeds were predominantly thermally induced, an even lower cutting speed (30 m/min) was selected to create mainly mechanically induced white layer.

For both materials the thrust force for the medium and high cutting speed was 45±5 N while for the lowest cutting speed the force was 75±5 N. The increased tool flank wear caused the thrust force for the martensitic material to increase to 250 N (low V_C), 132 N (medium V_C) and 104 N (high V_C). The thrust force for the bainitic materials with worn tool was 121 N (low V_C), 163 N (medium V_C) and 102 N (high V_C). Similar residual stress profiles were reported by Jacobson et al. [11] and Gunnberg et al. [3], who investigated the influence of the cutting speed on the surface integrity on bainitic steel and 18MnCr5 case carburized steel. They showed that increased cutting speed results in increased surface tensile residual stresses, which was related to the heat generated at the surface. Various researchers have stated that the primary reason for the compressive residual stresses in the white layer was due to the volume expansion associated with the phase transformation [7, 12]. However, Tönshoff et al. [4] showed that white layer formed predominantly due to phase transformation was accompanied by tensile residual stresses and increased retained austenite content. This is consistent with the results from the present investigation where the thermally formed white layers results in an increased retained austenite content and surface tensile residual stresses. Therefore, phase transformation solely resulting in volume expansion cannot be the main reason for the high compressive residual stresses in the white layer created by hard turning. This is also supported by the results obtained by Hosseini et al. [13] who studied the residual stresses and the retained austenite content in the white layer created during hard turning and wire electric discharge machining (W-EDM) in AISI 52100 steel. The white layer created during W-EDM was under high tensile residual stresses and contained ~30 vol. % of retained austenite. The white layer created during W-EDM is mainly due to phase transformation, which results in high retained austenite content and no compressive residual stresses due to lack of plastic deformation. The results from the present study show that predominantly mechanically formed white layer was accompanied by

compressive residual stresses and reduced retained austenite content. Similar results have been obtained by Ramesh et al. [8]. Therefore, it is believed that the white layers formed in samples M6 and B6 are due to severe plastic deformation allowing the strain-induced martensitic transformation to occur. The absence of dark layer under the white layer in samples M6 and B6 supports that the white layer formation is mainly due to mechanical work. The phenomena of strain-induced martensitic transformation have also been observed in for example shot-peened surfaces, where the martensitic transformation accelerates by the shot impact [14]. The approach of estimating the gradient in the retained austenite content with help of GIXRD allows a more precise interpretation of the white layer constituents and its formation mechanisms. In this investigation the gradient of the retained austenite content has been examined, which indicated that the distribution of the investigated phase is not homogenous. The measured retained austenite content can slightly vary due to the texture effects at the surface due to machining. However, initial TEM studies have shown only a slight preferred orientation. Also, the relationship between the $\varepsilon_{\Phi\psi}$ versus $\sin^2\psi$ was rather linear [15] during the residual stress measurements, indicating low crystallographic texture.

Based on the microstructure in the white layer, the surface temperature during machining has been estimated with the help of Time-Temperature-Austenitization (TTA) diagram. Even though, the contact pressure can affect the transition temperature, it has not been considered here when constructing the TTA-diagram. The temperature estimated is based upon rapid heating and rapid cooling. It has previously been shown that a contact pressure of ~3 GPa can influence the α-γ transition temperature by ~180˚C of iron [16]. However, Han et al. [17] estimated the temperature influence of only ~45˚C for AISI 1045 steel using Clausius-Clayperon equation with an effective stress on the material in the range of 350-700 MPa. The volume fraction of undissolved carbides in a fully spheroidized and annealed AISI 52100 steel containing 0.95 wt. % carbon is ~14.2 wt. %, having no carbon in the ferritic matrix [18]. After quenching the retained austenite content is ~15 vol. % and drops to ~2 vol. % after tempering [19]. The heat treatment resulting in the bainitic microstructure was designed to obtain less than ~1 vol. % of retained austenite. The final microstructure of the steels was characterized by ~4 wt. % of $(Fe,Cr)_3C$ carbides in a bainitic or martensitic structure with small volume fractions of retained austenite. Based upon the above mentioned correlation between the carbon and carbide content, formation of ~4 wt. % $(Fe,Cr)_3C$ carbides in the final microstructure requires ~0.25 wt.% carbon. According to the composition in Table 1, this gives a carbon content of ~0.7 wt. % in the matrix. Finally, considering the chemical composition of the steel and the microstructure the martensite start (M_S) temperature was estimated to be ~222˚C [20]. The transformation temperatures of ferrite-to-austenite ($\alpha \rightarrow \gamma$) Ac_1 (Ac_{1b}) and Ac_3 (Ac_{1e}), which are shown in the TTA-diagram are known to be influenced by the heating rate [21]. The TTA-diagram describes the phase transformation kinetics during austenitization at constant heating rates. Considering two different conditions with different heating rates: i) a fast heating (130˚C/s) up to 950˚C with a short austenitization time followed by quenching and ii) a moderate heating up to 860˚C and austenitization for a longer time followed by quenching [22]. The final microstructure in both cases consists of retained austenite (~12 vol. %), $(Fe,Cr)_3C$ (~4 vol. %) and martensite (~84 vol. %). The dashed line between Ac_1 and Ac_3 is an estimated temperature line based upon the two above mentioned cases. In machining, Shi and Liu [23] estimated the heating rate to be ~10^5˚C/s. Addressing the heating rate in the literature and two reference points combined with a reference line, the surface temperature can be estimated by the help of a TTA-diagram. In this particular case the surface temperature is estimated to be ~1200˚C. Chou [24] estimated the surface temperature to be ~1300˚C when he estimated the heating rate to be 10^6˚C/s by using Jeager's moving heat source theory. Our initial results indicate that the surface temperature is ~1200˚C assuming a heating rate of ~10^5˚C/s during white layer formation in hard turning. However, detailed temperature measurements and accurate heating rates are required for precise surface temperature determination. As mentioned earlier the effect of strain and pressure were not included in the TTA-diagram, which affects the transformation temperatures. The modified TTA-diagram was originally constructed for a martensitic microstructure [21]. However, as the austenitization temperature, carbide morphology and chemical composition were similar between the two investigated microstructures, the re-constructed TTA-diagram is applicable for both microstructures.

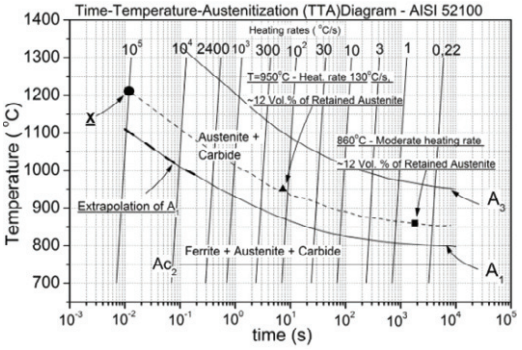

Fig. 6. TTA-diagram for AISI 52100 steel reconstructed and modified for this study from Atlas zur Wärmebehandlung der Stähle [21].

6. Conclusion

- The surface temperature during white layer formation in hard turning has been estimated to be ~1200˚C by using a modified TTA-diagram.
- At medium and high cutting speeds combined with high flank wear the increased retained austenite content and tensile residual stresses indicate that the white layer is predominantly thermally created.
- At the lowest cutting speed the reduced retained austenite content and the compressive residual stresses indicate that the formation of the white layer is mainly mechanically induced.
- Flank wear has a stronger influence on white layer formation than the cutting speed.
- Beneath the predominantly thermally formed white layer a dark layer is detected. No dark layer is observed in conjunction with mechanically created white layer.
- No significant carbide dissolution took place during white layer formation as the carbides were seen to be present in the differently created white layers.

Acknowledgement

The *Area of Advanced Production* at Chalmers is acknowledged for their financial support. The authors also acknowledge Dr. J. Alhström and Mr. S. Larsson for their help regarding the TTA-diagram and Mr. U. Jelvestam and Mr. F. Rhein for their contribution to the GIXRD measurements.

References

[1] Tonshoff, H. K., Arendt, C., Amo, R. Ben, Cutting of Hardened Steels, Annals of the CIRP, 2000;49/2:547–566.
[2] Abrao, A. M., Aspinwall, D. K., Tool Life and Workpiece Surface Integrity Evaluations When Machining Hardened AISI H13 and AISI E52100 Steels With Conventional Ceramic and PCBN Tool Materials, Wise, M. L. H., Society of Manufacturing Engineers, SME, MR95-195, 1995;1–9.
[3] Gunnberg, F., Escursell M., Jacobson, M., The influence of cutting parameters on residual stresses and surface topography during hard turning of 18MnCr5 case carburised steel J Mater Process Tech, 2006; 174:82–90.
[4] Tonshoff, H. K., Brandt, D., Wobker, H.-G., Potential and Limitation of Hard Turning, Society of Manufacturing Engineers, SME, MR95-215, 1995;1–14.
[5] Stead, J. E., Micro-Metallography and its Practical Application, J. West. Scot. Iron & Steel Inst., 1912;19:169–204.
[6] Griffiths, B. J., White Layer Formation at Machined Surfaces and Their Relationship to White Layer Formation at Worn Surfaces, J. Tribol., 1985;107:165–170.
[7] Thiele, J. D., Melkote, S. N., Peascone, R. A., Wathkins, T. R., Effect of Cutting-Edge Geometry and Workpiece Hardness on Surface Residual Stresses in Finish Hard Turning of AISI 52100 Steel, Trans. ASME, 2000;122:642–649.
[8] Ramesh, A., Melkote, S. N., Allard, L. F., Riester, L., Watkins, T. R., Analysis of White Layers Formed in Hard Turning of AISI 52100 Steel, J. Mater. Sci. Eng A., 2005;390:88–97.
[9] Akcan, S., Shah, S., Moylan, S. P., Chhabra, P. N., Chandrasekar S., Yang, H.T.Y., Formation of White Layers in Steels by Machining and Their Characteristics, Metall. Mater. Trans. A., 2002;33A:1245–1254.
[10] Thiele, J. D., Melkote, S. N., Effect of Tool Edge Geometry on Workpiece Subsurface Deformation and Through Thickness Residual Stresses for Hard Turning of AISI 52100 Steel, Journal of Manufacturing Processes, 2000;2/4:270–276.
[11] Jacobson, M., Dahlman, P., Gunnberg, F., Cutting Speed Influence on surface Integrity of Hard Turned bainitic Steel, J. Mater. Process. Technol., 2002;128:318–323.
[12] Liu, C. R., Barash, M. M., The mechanical state of the sublayer of a surface generated by chip-removal process – Part II, Trans. ASME, 1976;98/4:1202–1208
[13] Hosseini, S. B., Klement, U., Kaminski, J., Microstructure Characterization of White Layer Formed by Hard Turning and Wire Electric Discharge Machining in High Carbon Steel (AISI 52100), TTP, Switzerland, 2012;409:684–689
[14] Totten, G., Howes, M., Inoue, T., Handbook of Residual Stress and Deformation of Steel, ASM International, Materials Park, OH, 2002;447–448.
[15] S. B. Hosseini, B. Karlsson, T. Vuoristo, K. Dalaei, Determination of Stresses and Retained Austenite in Carbon Steels by X-rays – A Round Robin Study, Experimental Mechanics, 2011;51:59–69.
[16] Darken, L. S., Gurry, R. W., Physical Chemistery of Metals, McGraw-Hill, 1953,
[17] S. Han, S. N. Melkote, M. S. Haluska, T. R. Watkins, White Layer Formation due to Phase Transformation in Orthogonal Machining of AISI 1045 Annealed Steel, J. Mater. Sci. Eng A., 2008;488:195–204.
[18] Beswick, J. M., The effect of chromium in high carbon bearing steels, Metall. Mater. Trans. A, 1987;18A:1897–1906.
[19] Banarjee, R. L., X-ray Determination of Retained Austenite, J. Heat. Treat., 1981;2/2:147–149.
[20] Andrews, K. W., Empirical formulae for the calculation of some transformation temperatures, JISI, 1965;203:721–727.
[21] Orlich, J., Rose, A., Wiest P., Atlas zur Wärmebehandlung der Stähle, Band 3, Max-Planck-Institut für Eisenforschung: Verlag Stahleisen Düsseldorf. 1973;176.
[22] Melander, M., Theoretical and Experimental Study of Stationary and Progressive Induction Hardening, J. Heat. Treat., 1985;4/2:145–166.
[23] Shi, J., Liu, C. R., The Influence of Materials Models on Finite Element Simulation of Machining, J. Manuf. Sci. Eng, 2004;126:849–857.
[24] Chou, Y. K.., Surface Hardening of AISI 4340 Steel by Machining: A Preliminary Investigation, J. Mater. Process. Technol, 2002:124;171-177